SURVEY OF MR IMAGE PROCESSING METHODS

László LEFKOVITS[1] Szidónia LEFKOVITS[2] Mircea Florin VAIDA[3]
[1]*Sapientia University, Tîrgu-Mureş(Corunca) şos. Sighişoarei 1C, Tel. +40 265 206 210, lefkolaci@ms.sapienta.ro*
[2]*"Petru Maior" University, Tîrgu-Mureş, N. Iorga nr.1, Tel. +40 265 262 275, szidonia.lefkovits@science.upm.ro*
[3]*Technical University of Cluj-Napoca, Memorandumului 28, Tel. +40264 401 810, mircea.vaida@com.utcluj.ro*

Abstract: In this paper a synthesis of the main concepts and the most important MRI image acquisition and processing methods are presented. These two processes are clearly delimited, without any interference in our research means. The magnetic resonance acquisition methods are the exclusive tasks of medical equipment provider companies. The image processing methods – inhomogeneity correction, segmentation, registration and digital atlases – fall on the software developers. The starting points of such a system are the multimodal MR images. The purpose of these methods is the precise delimitation of anatomic structures and determination of benign and malign tissues. The goal of the research is to offer to medical experts a useful knowledge to combine the methods optimally and to obtain better medical results in assisted diagnosis.

Keywords: *MRI, inhomogeneity, segmentation, registration, digital atlases.*

I. INTRODUCTION

The analysis and interpretation of medical images are the radiologist's task. Surgery will greatly facilitate their work by automatic or semi-automatic image processing technologies. There are many software tools that help identify anatomical structures and forms, differentiate benign and malignant tissues, determine the exact size and localization of organs and recognize different conditions for the organism to function properly.

Medical images are obtained through the interaction of a physical factor with the organism. The measured parameters of physical factors are altered differentially according to different tissues. Specialized sensors convert the signals received into digitally coded information that constitutes the basis of software processing. A usual way to present this information is the visualization in gray scale or artificially colored images. The quality of the images depends on the sensitivity and resolution of the sensors. Modern medical imaging techniques must make use of the advantages offered by the newest developments in computer technology.

I.1 THE MRI ACQUISITION PROCESS

The MRI acquisition process is based on several important discoveries [25]:

- protons – essentially, small magnets – align themselves in the direction of an external strong magnetic field – discovered in 1937 by Isidor Isaac Rabi (Nobel Prize in 1944)
- the nuclear magnetic resonance phenomenon –which means that in a given magnetic field, atom nuclei absorb and reemit electromagnetic radiation. – discovered in 1946 by Edward Purcell and Felix Bloch (Nobel Prize 1952).
- the proton magnetic field processes with Larmor frequency ($v=\gamma B$ - γ is the gyromagnetic ratio and B is the magnitude of the magnetic field) around the external field.
- the frequency of the magnetic field can precisely encode the spatial position of the nuclei – established by Paul C. Lauterbur and Sir Peter Mansfield in 1973 (Nobel Prize in 2003).
- achievements in pulsed Fourier Transform with application in MRI were made by Richard Ernst in 1991 (Nobel Prize in 1992).

The spectra of the reemitted electromagnetic radiation determine the spatial density of protons, and the chemical composition of the analyzed matter can only be deduced indirectly. Biological tissues are characterized by high water content and therefore the concentration of hydrogen atoms can be measured easily. In short, if a magnetic field is generated which is different in each spatial position, the distribution of the hydrogen nuclei concentration can be extracted from the signal spectrum intensity. Such magnetic fields can be obtained with the use of well-designed coils and with computer-derived currents (Figure 1). The excitation electromagnetic fields are emitted by RF antennas, and the same antennas measure the response signal [1]. These responses are time-sampled and create the so-called raw image.

Each frequency component from the row image corresponds to a well-defined point in space, and its amplitude is proportional to the concentration of hydrogen nuclei. This space is called the K-space. Applying the inverse Fourier transform to the k-space, a visible image, the weighted PD proton density image, is obtained [7].

The magnetic resonance phenomenon can be measured after the excitation of radio wave stops. Information concerning the analyzed tissue is obtained not only from the proton density image but also from the measurement of the response decay. The time constant which describes how parallel magnetization returns to its equilibrium value is called the spin-lattice relaxation time, T1. The time constant that describes the return to equilibrium of the transverse magnetization is called the spin-spin relaxation time, T2. These parameters are independent and tissue specific [16]. Accordingly, the most frequently used MR images are (Figure 1. –one slice vector image with tumor published for MICAI 2012 competition [2]):

Manuscript received October 27, 2014; revised December 11, 2014

- T1-weighted images – normal anatomical structures: the cerebrospinal fluid is dark;
- T2-weighted images – moderately pathological images: the cerebrospinal fluid is white, the white matter is dark;
- PD-proton density images – the cerebrospinal fluid is very clear, gray matter is brighter than the white matter.

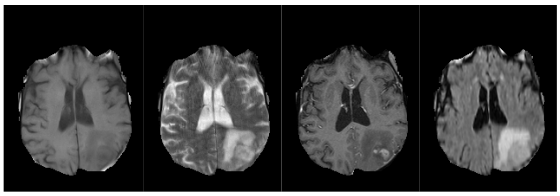

Figure 1. MR images: T1, T2, T1C, FLAIR[2]

The operating principle of MR image acquisition and processing can be seen in Figure 2. Spatial sampling is driven by pulse sequences, creating the optimal gradient field. The electromagnetic resonance is measured by RF antennas, and the signal derived is sampled temporally and saved in raw images. Sequences of such images build the "K-space". In the K-space, the spatial information is phase- and frequency-encoded. Signal processing techniques and the inverse Fourier transformation translate the K-space into visible image sequences, usually saved in a standard format.

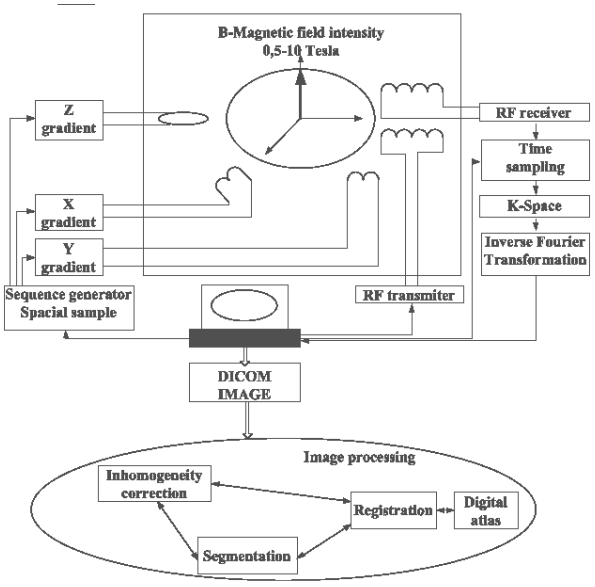

Figure 2. MRI acquisition and processing

This image acquisition process is offered by equipment manufacturer companies. Users can apply only some well-defined procedures in image acquisition, but cannot modify them. Even the row images remain proprietary to the manufacturer. We can perform further image processing by using the Dicom images provided by the equipment. In the following chapters, we shall present several methods of image processing which are treated separately, yet have a strong connection.

II. MR IMAGE INHOMOGENEITY

The main feature of MR images is the relation of the same intensity values to the same tissue regardless of their spatial location. Unfortunately, the image processing is greatly affected by the changes in intensity. The literature defines the inhomogeneity of MR image intensity by the variation of the voxel intensities for the same tissue. This inhomogeneity affects the whole image. The homogeneous image is an ideal theoretical image where the same intensity corresponds to the same tissue. The difference between the original image and the homogeneous image is called the bias image. This image is approximately constant, with slightly varying intensity over the image and very low frequencies (Figure 3).

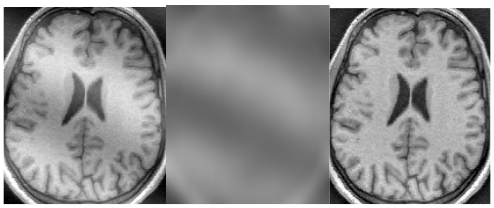

Figure 3. MR images: real, bias, corrected

The human visual system removes this inhomogeneity automatically. Conversely, machine vision is greatly influenced by the changes in the intensity of the images. The goal of automatic image processing is accurate detection, localization and separation of the shape of specific tissues, and sometimes the discovery of details hidden from the human eye. In order to obtain suitable image processing, it is necessary to eliminate the inhomogeneity using correction procedures. It is important to remove only that type of noise without modifying the useful information of the image.

The inhomogeneity comes from the imprecision of the recorder or from the interaction of the analyzed subject with the strong magnetic field. The errors produced by the recording equipment result from: the non-linearity of the static magnetic field or of the gradient field, the non-linear variation of the coil current, and the limited bandwidth of the transmission/reception channels. These factors are stable and reproducible, and can be minimized with adequate equipment calibration. The shape and magnetic properties of the subject scanned modifies the linearity of the magnetic field. This inhomogeneity varies from subject to subject, making correction by hardware calibration alone almost impossible.

II.1 MODELS OF INTENSITY INHOMOGENEITY

Intensity inhomogeneity is modeled according to the correction methods used. The model assumes that intensity inhomogeneity is additive or multiplicative. The additive form comes from the superposition of the magnetic field, while the multiplicative form originates from the sensitivity of the reception coils. Assume the following notations: $u(x)$ - the inhomogeneity-free image; $b(x)$ - the bias image; $n(x)$ - the noise image; $v(x)$ - the captured real image. Accordingly, the most frequently used models are:

1. The multiplicative model with additive Gaussian noise independent from image information [28] $v(x) = u(x)\cdot b(x) + n(x)$, where $n(x)$ Gaussian noise.
2. The multiplicative model with biological noise [6] $v(x) = \left(u(x) + n(x)\right)\cdot b(x)$.
3. The logarithmic model with additive Gaussian noise [15]

$v(x) = \log u(x) + \log b(x) + n(x)$, where *n(x)* Gaussian noise, but different from the first model.

II. 2 CORRECTION METHODS

Inhomogeneity correction procedures that consider the bias of the source are prospective and retrospective methods [33]. Prospective methods eliminate the nonlinearities caused by hardware equipment. There are many procedures provided by the equipment manufacturers:

- using phantoms with known physical properties and calibrated images;
- the choice of adequate surface or volume coils;
- the application of different special sequences.

Retrospective methods reduce the perturbation caused by the biological sources. These methods are based only on image intensities and prior knowledge. These procedures are based on one main feature of pixel intensities. Such properties can be:

- image filtering in frequency domain [9, 18];
- surface matching [10, 32];
- segmentation-based methods [14, 20, 30];
- histogram-based methods [23, 34, 29, 32].

The most popular method is the N3 nonparametric nonuniform intensity normalization, correction method, developed by J. Sled [29]. The N4 method a new variant of the N3 algorithm is proposed by N. J. Tustison [32]. Each algorithm is based only on assumptions of the bias image pixel intensity distribution, without any consideration on image information and prior knowledge.

II.3 CORRECTION EVALUATION

Inhomogeneity correction methods can be tested according to different criteria in order to evaluate their effectiveness, advantages, disadvantages and application. We can make quantitative and quality measurements. Quality evaluation is based on the human eye, therefore being based on various comparisons. The quality can take into account differences between:

- the intensity of the bias image;
- hand-marked pixels;
- the resulting homogeneity;
- the rendered surface;
- the segmentation result;
- the histograms of bias and corrected images.

The quantitative evaluation is quantified, but remains relative because there are no comparison criteria in the form of the images adopted. This evaluation is based on specific measurements and formulas. The most frequently used measurements are the following:

The difference between the bias images intensities is given by the squared error (RMS Root Mean Square) [18]:

$$rms(b_1(x), b_2(x)) = \sqrt{\sum_{x\in\Omega} \left(b_1(x) - b_2(x)\right)^2 / n} \quad (1)$$

The correlation coefficient is a result of direct comparisons and, in this case, it is not necessary to normalize the images. Unfortunately, however, this does not apply to inhomogeneous noisy images, so it is necessary to manually mark areas with constant intensity, supposing that these are homogeneous.

Image inhomogeneity can also be characterized by the standard deviation and the mean of pixel intensities. Supposing a constant intensity in a certain tissue, the mean value does not change, but in the corrected image, both the standard deviation and the coefficient of variation decrease. The coefficient of variation *CV* is the ratio between the standard deviation and the mean for the same tissue: $CV = \sigma(\mathrm{I})/\mu(I)$, where *I* are pixel intensities of one given tissue. The disadvantage of *CV* is the sensitivity regarding the changes in the average value. The *CV* changes with the average value, at a given standard deviation.

To eliminate this disadvantage, we can use the joint variation coefficient *JVC*, to evaluate the inhomogeneity between two classes:

$$JVC\left(S_1, S_2\right)) = \sigma(\mathrm{S}_1) + \sigma(\mathrm{S}_2) / \mid \mu(\mathrm{S}_1) - \mu(\mathrm{S}_2) \mid \quad (2)$$

where *S1* the number of voxels belonging to a given tissue and *S2* the number of voxels belonging to another tissue.

Currently, two coefficients, used for segmentation evaluation, can be applied in correction evaluation:

-Jaccard similarity [12]

$$J(S_1, S_2) = \mid S_1 \cap S_2 \mid / \mid S_1 \cup S_2 \mid \quad (3)$$

-Ditze coefficient [21]

$$J(S_1, S_2) = 2 \cdot \mid S_1 \cap S_2 \mid / (\mid S_1 \mid + \mid S_2 \mid) \quad (4)$$

where *S1* the number of voxels belonging to a given class and *S2* the number of voxels belonging to the ideal segmentation (gold standard).

These evaluations remain relative as long as we do not have a completely uniform, perfect image. The segmentation could solve the issue of inhomogeneity, but correct segmentation is not possible to obtain because it is altered by inhomogeneity. One possible solution could be obtained by applying digital atlases, which offer the gold standard segmentation. In order to use the high-resolution atlases, a precise registration of the target images is necessary.

III. REGISTRATION AND FUNCTIONAL LOCALIZATION

The registration brings the images from a given subject to the same form. The registration is a complicated process which can be divided into four components [13] (Figure 4).

- landmarks – anatomically equivalent pair of points must be defined on the registered images. The external points are determined by the head-fixing equipment or are referred to the skull, but these markers have to be detected by the registration system.
- the transformation – it is a (mainly nonlinear) rigid transformation [26, 17, 11]. The complexity of the system is determined by the number of parameters used. If every voxel in a given volume containing *N* voxels is transformed, then a maximum of *9N* parameterized transformations can be defined.

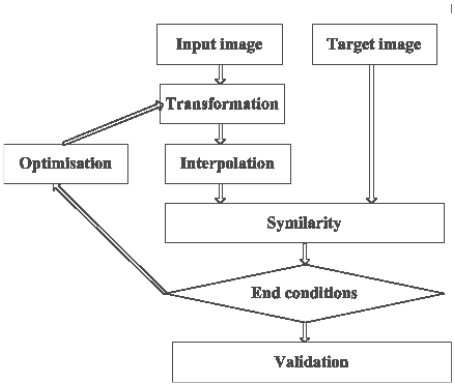

Figure 4. Registration process

• optimization – its goal is to maximize the similarity between the sample image and the transformed image. The quality of the registration is defined by an objective function measuring the similarity.
• interpolation – in general, the destination image is a high-quality, high-resolution image, and thus the resolution of the source image has to be converted to the same quality. This can be achieved by resampling and interpolation algorithms.
In order to evaluate MR images individually or based on a population, the convertibility between different image types must be ensured (example: PET, SPECT, CT, fMRI, BLOOD).
In case of individual examination, it is sufficient to perform motion correction, but in case of population analysis, brain atlas techniques are used.
Brain atlases are usually obtained in two steps:
• the first is registration – here, a transformation has to be defined that allows the records to be put into an anatomically similar space, according to the reference images.
• the second is functional localization – here, functional labels are added to the voxels.
Functional localization is classified by the source and result images in [13]
• subject to template;
• subject to atlas;
• functional image to atlas.
Similarly, the registration is also defined by the source and result image. Multimodal registration of the same person can be achieved by simple affine transformations. For this, a rigid transformation [27] defined by 12 parameters (shifting, rotating, scaling and distortion) is needed. The transformation can be global if it is applied on the whole image, or it can be local if it is computed by the sum of local linear part-transformations.

IV. DIGITAL BRAIN ATLASES

Physicians evaluate medical images relatively quickly. They are able to see things which can only be discovered by medical experts. The diagnosis is the result of a long learning process and is supplemented by a lot of practical experience. The goal of atlases is the unification of the numerous diagnoses and pooling all the experience. Discovering RMI brain image registration supplemented existing brain atlases with other valuable medical information. The digital brain atlas is a complex database which stores anatomically precise images and the local knowledge associated with them. The atlases store anatomical structures mainly in the form of digital images, but they can contain functional, temporal, morphological, pathological, statistical and genetic information as well.
Typical applications:
• diagnostics – the damage to the areas of the brain (Alzheimer's disease, multiple sclerosis, tumor, stroke, speech issues, dyslexia etc.);
• anatomical functional localization – the functional images are registered by adding descriptive information to a brain atlas;
• surgery plan – useful information can be gained from the possible circumstances and risks of the intervention planned;
• education – spectacular 3D reconstructions can be obtained from the brain images;
• segmentation algorithms – segmentation based on atlases, algorithm testing, benchmarks.

IV.1 COORDINATE SYSTEMS AND. TEMPLATES

In order to compare different MR images, a well-defined coordinate system is needed. A transformation method through which the brain images of every subject can be transformed into a given coordinate system, enabling the comparison of two images, is also necessary. The most widespread coordinate system is the Talairach stereo-taxic (symmetric) system [31]. In this system, the origin is the anterior commissure point. The *Oy* axis crosses the posterior commissure point. The *zOy* plane is the best plane which separates the two hemispheres. Accordingly, the *Oz* axis is perpendicular to the *Oy* axis and it is oriented downward. The *Ox* axis is defined by a line crossing the origin, which is perpendicular to the *yOz* axis. Thus obtained, coordinate axes cross the skull in 6 points. These 6 points and the two commissure points define 8 reference points. The planes of the coordinate system and the plane parallel to the *xOz* and crossing the posterior commissure point cut the volume of the brain into 12 parts. The uniform fitting of the 8 points determine the affine transformation of the 12 parts. These conditions assure a uniform registration [31].

In order to analyze the population, an average brain has to be marked. The first such atlas was developed in the Brain Imaging Center of the Montreal Neurological Institute (MNI) based on 305 T1-weighted MR images [6]. The individual MRIs were projected onto the Talairach coordinate system by using an interactive software. The images recorded were normalized according to the voxel intensities, and by computing a mean, they managed to obtain the Montreal MNI brain atlas template. Certain transformations ensure the interoperability between the Talairach system and anatomical MNI space. The most important digital brain atlases can be used freely on the internet [3, 4, 5].

IV.2 BRAIN ATLAS TYPES

Brain atlases consist of several high resolution maps; these correspondences to neurological information stored in a digital volume, in different ways. The MR multimodal images assign to a voxel *x* a gray-scale image I(x): $\mathbf{R}^3 \rightarrow \mathbf{R}^N$, where $\mathbf{R}^3$ the space of voxel coordinates and $\mathbf{R}^N$ are the different *N* intensity images.
Based on the information stored, the most well-known brain atlas types are:
• label map: consists of a digital voxel and the corresponding description file. The voxel intensity from a given volume corresponds to an index which is assigned to a neurological entry. The mapping is at a one-one relation.
• hierarchical label map: more neurological information can be assigned to a voxel. More voxel indexes can be obtained if all the voxels are retrieved corresponding to a given condition. The assignment is not unique, so the relation is one to *n*. If only one type of atlas is used, then the intensity values are denoted by $\pi^i(x)$ and the corresponding entries are $\pi^L(x)$, where L is the set of classes $\mathrm{L}=\{1,2,...,c\}$ and c is the number of classes. The topological atlases are defined as:

$$\pi^i : x \in \mathbf{R}^3 \rightarrow \pi^i(x) \in \mathbf{R} \quad (5)$$

$$\pi^L : x \in \mathbf{R}^3 \rightarrow \pi^L(x) \in \mathrm{L} \quad (6)$$

• probability map: one voxel contains the probability

according to single neurological information. For example, the probability map of gray matter determines the probability of a voxel being gray matter.

- the maximum probability map is built from one label map and more probability maps. The label map assigns the localization to the most probable information, and the probability can be obtained from the probability map corresponding to that location. The maximum probability map determines the most probable neurological information and its probability in a particular location [35].

In case of probability maps, the density function $\pi_c^P(x)$ referring to a given class can be defined for every c class, assuming $\int \pi_c^P(x)dx = 1$. The probability map is defined by the following system:

$$\pi^i : x \in \mathbf{R}^3 \to \pi^i(x) \in \mathbf{R} \quad (7)$$

$$\pi_c^P : x \in \mathbf{R}^3 \to \pi_c^P(x) \in \mathbf{R} \quad (8)$$

V. ATLAS-BASED SEGMENTATION

Segmentation is the geometrical separation of foreground and background points, which in fact means the separation of the objects from the background. Prior knowledge significantly influences recognition performance. This means that digital brain images represent new possibilities in brain segmentation. Assuming there was a perfect atlas, quality of segmentation would only depend on the registration of the image to be segmented. With regard to atlas types, there are three segmentation methods:

- simple label propagation – here, only one template is used. The result of the segmentation is simply the $S(x)=\pi^L(\tau(x))$ relation, where τ is the segmentation transformation, which converts the image space to the template space $\tau : \mathbf{R}^3 \to \mathbf{R}^3$ [8].
- voting-based label propagation – in this case, more templates are used. A decision algorithm which selects the best label based on a given criteria is needed [22]. The formulae of the segmentation are the following:

$$S(x) = \arg\max_c \sum_{i=1}^{P} w_i(x) \cdot f\left(\pi_i^L\left(\hat{\tau}_i(x)\right), c\right) \quad (9)$$

where c represents the classes, P the number of atlases and w_i is the weight of atlas and f is the similarity function:

$$f\left(\pi_i^L\left(\hat{\tau}_i(x)\right), c\right) = \begin{cases} 1, \text{ ha } \pi_i^L\left(\hat{\tau}_i(x)\right) = c \\ 0, \text{ ha } \pi_i^L\left(\hat{\tau}_i(x)\right) \neq c \end{cases} \quad (10)$$

- probability-based segmentation: this type of segmentation determines the probability of voxels belonging to a class. These probabilities can be easily implemented in the Bayes model:

$$S(x) = \arg\max_c p\left(I(x) \mid c\right) \cdot p(c) \quad (11)$$

where $p\left(I(x) \mid c\right)$ is the conditional probability of $I(x)$ with respect to class c, and $p(c)$ is the probability of class c. These conditional probabilities can also be applied in conditional models $S(x) = \arg\min_c \left(E_d + \lambda E_s\right)$, where the segmentation is, in fact, an energy minimization: where E_d is the energy term, and λ is the regularization coefficient of the smoothed energy E_S. Here, segmentation requires the $p(I(x)|c)$ and $p(c)$ probabilities, which can be determined by the Gaussian Mixture Model or parametric estimation. Brain atlases help the early discovery of brain damage and more accurate tracking of diseases.

VI. CONCLUSION AND FURTHER IMPROVEMENTS

This paper presents the most important image processing methods such as inhomogeneity correction, segmentation and registration (Figure 2.). Each one of these methods solves a difficult image processing issue on its own. If we look at them carefully, important relations can be discovered among them. Good segmentation supposes a noiseless image; registration supposes accurate segmentation, and the noise and inhomogeneity from the registered image can be easily filtered. Thus, we have a vicious circle: how do we select the initial method? Generally, modern systems combine two of these methods iteratively. C. Li demonstrates the possibilities to eliminate inhomogeneity by using the level set segmentation method [19]. A. Mayer creates an adaptive mean shift clustering framework to segment and simultaneously correct inhomogeneity in MR images [24]. An efficient segmentation with noise and inhomogeneity reduction is possible by using c-means fuzzy clustering [30]. But in all these works, authors proved their method on various images without comparing their result with other methods or benchmark segmentation. One possibility is offered by registering one set RM images with a given atlas or template in order to compare the segmentation results. The comparison is even more difficult because the prosed methods are not implemented in the same framework and these applications are not open source. Each method has its own inputs and outputs which have to be standardized in order to compare them. Currently we are working on the comparison of inhomogeneity reduction of the above mentioned methods with the N4 widely accepted algorithm [32], available in the ITK package [36]. The question is how to improve these methods with apriori knowledge offered by digital atlases. The goal is to combine the methods optimally and set the correct stop conditions, or if possible, combine them in a unique, automated framework. This approach is still an open question. The MRI helps radiologists to give the right diagnosis and the precise image segmentation is indispensable in surgery planning.

ACKNOWLEDGEMENT

The work of László Lefkovits in this paper is supported by The Sectorial Operational Program Human Resources Development POSDRU/159/1.5/S/137516 financed by the European Social Found and by the Romanian Government. Financial support of the work of Szidónia Lefkovits was provided from programs co-financed by The Sectorial Operational Program of Human Resources Development, Investing in people! Key Area of Intervention 1.5 "Doctoral and Postdoctoral scholarship in support of research", Project title: "Integrated system for quality improvement of the doctoral and post-doctoral research in Romania and promoting the role of science in society", Contract: POSDRU/159/1.5/S/133652.

REFERENCES

[1 Joseph P. Hornak. The Basics of NMR, Publisher Rochester Institute of Technology 1999, ebook online: http://www.cis.rit.edu/htbooks/nmr/inside.htm [Accessed 2014]

[2] BraTS Multimodal Brain Tumor Segmentation Challenge http://www2.imm.dtu.dk/projects/BRATS2012/data.html [Accessed 2014]
[3] Laboratory of Nuro Imaging LONI Atlasses http://www.loni.usc.edu/atlases/ [Accessed 2014]
[4] Laboratory of Nuro Imaging LONI http://www.loni.usc.edu [Accessed 2014]
[5] Simulated Brain Database http://www.bic.mni.mcgill.ca/brainweb/ [Accessed 2014]
[6] J. Ashburner and K. J. Friston. Unified segmentation. NeuroImage, 26(3):839 –851, 2005.
[7] Abiodun M. Aibinu, Momoh J. E. Salami, Amir A. Shafie and Athaur Rahman Najeeb MRI Reconstruction Using Discrete Fourier Transform: A tutorial, World Academy of Science, Engineering and Technology, Vol:2 2008-06-29
[8] A. Oliver, X. Lladó, J. Freixenet, and M. Bach Cuadra. A review of atlas-based segmentation for magnetic resonance brain images. Comput. Methods Prog. Biomed., 104(3):158–177, Dec. 2011
[9] M. S. Cohen, R. M. DuBois, and M. M. Zeineh. Rapid and effective correction of rf inhomogeneity for high field magnetic resonance imaging. Human Brain Mapping, 10(4):204–211, 2000.
[10] B. Dawant, A. Zijdenbos, and R. Margolin. Correction of intensity variations in MR images for computer-aided tissue classification. Medical Imaging, IEEE Transactions on, 12(4):770–781, Dec 1993.
[11] J. C. Gee and D. R. Haynor. Chapter 6 - numerical methods for high-dimensional warps. In W. Toga, editor, Brain Warping, pages 101 – 113. Academic Press, San Diego, 1999.
[12] G. Gerig, M. Prastawa, W. Lin, and J. Gilmore. Assessing early brain development in neonates by segmentation of high-resolution 3t MRI. In R. Ellis and T. Peters, editors, Medical Image Computing and Computer-Assisted Intervention MICCAI 2003, volume 2879 of Lecture Notes in Computer Science, pages 979–980. Springer Berlin Heidelberg, 2003.
[13] A. Gholipour, N. Kehtarnavaz, R. Briggs, M. Devous, and K. Gopinath. Brain functional localization: A survey of image registration techniques. Medical Imaging, IEEE Transactions on, 26(4):427–451, April 2007.
[14] J. D. Gispert, S. Reig, J. Pascau, J. J. Vaquero, P. García-Barreno, and M. Desco. Method for bias field correction of brain t1-weighted magnetic resonance images minimizing segmentation error. Human Brain Mapping, 22(2):133–144, 2004
[15] R. Guillemaud and M. Brady. Estimating the bias field of MR images. Medical Imaging, IEEE Transactions on, 16(3):238–251, June 1997.
[16] M. A. Griswold, P. M. Jakob, M. Kotas, V. Gulani, M. Flentje, A. Haase, Inversion Recovery TrueFISP: Quantification of T1, T2, and Spin Density, Magnetic Resonance in Medicine 51:661–667 (2004)
[17] G. Hermosillo, C. Chefd'Hotel, and O. Faugeras. Variational methods for multi-modal image matching. International Journal of Computer Vision, 50(3):329–343, 2002.
[18] E. B. Lewis and N. C. Fox. Correction of differential intensity inhomogeneity in longitudinal {MR} images. NeuroImage, 23(1):75 – 83, 2004.
[19] C. Li, R. Huang, Z. Ding, J. Gatenby, D. Metaxas, and J. Gore. A level set method for image segmentation in the presence of intensity inhomogeneities with application to mri. Image Processing, IEEE Transactions on, 20(7):2007–2016, July 2011.
[20] X. Li, L. Li, H. Lu, and Z. Liang. Partial volume segmentation of brain magnetic resonance images based on maximum a posteriori probability. Medical Physics, 32(7):2337–2345, 2005.
[21] A.-C. Liew and H. Yan. An adaptive spatial fuzzy clustering algorithm for 3-d MR image segmentation. Medical Imaging, IEEE Transactions on, 22(9):1063–1075, Sept 2003
[22] P. Lorenzen, B. C. Davis, and S. Joshi. Unbiased atlas formation via large deformations metric mapping. In J. S. Duncan and G. Gerig, editors, Medical Image Computing and Computer Assisted Intervention MICCAI 2005, volume 3750 of Lecture Notes in Computer Science, pages 411–418. Springer Berlin Heidelberg, 2005.
[23] J.-F. Mangin. Entropy minimization for automatic correction of intensity nonuniformity. In Mathematical Methods in Biomedical Image Analysis, 2000. Proceedings. IEEE Workshop on, pages 162–169, 2000.
[24] A. Mayer and H. Greenspan. An adaptive mean-shift framework for mri brain segmentation. Medical Imaging, IEEE Transactions on, 28(8):1238–1250, Aug 2009.
[25] D. Weishaupt, V. D. Köchli, B. Marincek, How Does MRI Work? ISBN-10 3-540-30067-8 Springer Berlin Heidelberg New York
[26] V. Pekar and E. Gladilin. Deformable image registration by adaptive gaussian forces. In M. Sonka, I. Kakadiaris, and J. Kybic, editors, Computer Vision and Mathematical Methods in Medical and Biomedical Image Analysis, volume 3117 of Lecture Notes in Computer Science, pages 317–328. Springer Berlin Heidelberg, 2004.
[27] S. Periaswamy and H. Farid. Elastic registration in the presence of intensity variations. Medical Imaging, IEEE Transactions on, 22(7):865–874, July 2003.
[28] D. W. Shattuck, S. R. Sandor-Leahy, K. A. Schaper, D. A. Rottenberg, and R. M. Leahy. Magnetic resonance image tissue classification using a partial volume model. NeuroImage, 13(5):856 – 876, 2001.
[29] J. Sled, A. Zijdenbos, and A. Evans. A nonparametric method for automatic correction of intensity nonuniformity in MRI data. Medical Imaging, IEEE Transactions on, 17(1):87–97, Feb 1998.
[30] L. Szilágyi, D. Iclănzan, L. Crăciun, and S. M. Szilágyi. An efficient approach to intensity inhomogeneity compensation using c-means clustering models. In C. San Martin and S.-W. Kim, editors, Progress in Pattern Recognition, Image Analysis, Computer Vision, and Applications, volume 7042 of Lecture Notes in Computer Science, pages 312–319. Springer Berlin Heidelberg, 2011.
[31] J. Talairach and P. Tournoux. Co-Planar Stereotaxic Atlas of the Human Brain: 3-D Proportional System: An Approach to Cerebral Imaging (Thieme Classics) . Thieme, jan 1988.
[32] Tustison, N. J., Avants, B. B., Cook, P. A., Zheng, Y., Egan, A., Yushkevich, P. A., and Gee, J. C. N4ITK: improved N3 bias correction. Medical Imaging, IEEE Transactions on, 29(6), 1310-1320, 2010.
[33] U. Vovk and B. Likar. A review of methods for correction of intensity inhomogeneity in MRI. Medical Imaging, IEEE Transactions on, 26(3):405–421, March 2007.
[34] U. Vovk, F. Pernuš, and B. Likar. Intensity inhomogeneity correction of multispectral MR images. NeuroImage, 32(1):54 – 61, 2006.
[35] L. Zőllei, E. Learned-Miller, E. Grimson, and W. Wells. Efficient population registration of 3D data. In Y. Liu, T. Jiang, and C. Zhang, editors, Computer Vision for Biomedical Image Applications, volume 3765 of Lecture Notes in Computer Science, pages 291–301. 2005.
[36] http://www.itk.org/itkindex.html, Insight Segmentation and Registration Toolkit